Biomol NMR Assign
DOI 10.1007/s12104-013-9503-5

ARTICLE

NMR assignments of PI3-SH3 domain aided by protonless NMR spectroscopy

Shang-Te Danny Hsu

Received: 6 April 2013 / Accepted: 29 June 2013

Abstract We report here the near complete assignments of native bovine PI3-SH3 domain, which has been a model system for protein folding, misfolding and amyloid fibril formation. The use of ^{13}C-detected protonless NMR spectroscopy is instrumental in assigning the spin system of the proline residue at the C-terminus in addition to the missing resonances in proton-based NMR spectra due to rapid solvent exchange. It also helps assign the resonances of all three proline amine nitrogen nuclei, which are underrepresented in the database. Comparison of the backbone ^{13}C resonances of PI3-SH3 in its native and amyloid fibril states shows that the aggregation of PI3-SH3 is accompanied by major conformational rearrangements.

Keywords PI3-SH3 · Protein misfolding · Amyloid · Protonless NMR spectroscopy

S.-T. D. Hsu (✉)
Department of Chemistry, University of Cambridge, Lensfield Road, Cambridge CB2 1EW, UK
e-mail: sthsu@gate.sinica.edu.tw

S.-T. D. Hsu
Institute of Biological Chemistry, Academia Sinica, 128, Section 2, Academia Road, Taipei 11529, Taiwan

S.-T. D. Hsu
Institute of Biochemical Sciences, National Taiwan University, 1, Section 2, Roosevelt Road, Taipei 10617, Taiwan

S.-T. D. Hsu
Institute of Bioinformatics and Structural Biology, National Tsing Hua University, 101, Section 2, Kuang-Fu Road, Hsinchu 30013, Taiwan

Biological context

The bovine SH3 domain of the p85α subunit of phosphatidylinositol-3-OH kinase (PI3-SH3) is one of the most studied model systems for protein folding, misfolding and amyloid fibril formation (Bayro et al. 2010; Guijarro et al. 1998a, b; Jimenez et al. 1999; Orte et al. 2008). PI3-SH3 exhibits increased aggregation propensity under acidic conditions and readily aggregates into typical amyloid fibril structures (Jimenez et al. 1999; Zurdo et al. 2001). It contains a 22-residue n-src loop that is much longer than that of most SH3 domains. By grafting part of the elongated n-src loop of PI3-SH3 into a non-amyloidogenic SH3 domain, the chimeric SH3 domain also aggregates into amyloid fibrils, indicating that the n-src loop of PI3-SH3 is highly amyloidogenic (Ventura et al. 2002). The solution structures of PI3-SH3 have been reported previously using ^{15}N-labelled samples (PDB entries 1PNJ, 2PNI, 2PKS and 2PKT) (Booker et al. 1993; Koyama et al. 1993a, b). Its structure has also been determined by X-ray crystallography (PDB entry 1PHT) (Liang et al. 1996). ^{1}H NMR spectroscopy has been employed to investigate the folding and misfolding of PI3-SH3 (Guijarro et al. 1998b; Zurdo et al. 2001). Recently, a solid state NMR study showed that the amyloid form of PI3-SH3 contains four extended β-strands in the well-ordered fibril core and that the β-strand registering differs significantly from that of the native structure in solution, indicating conformational rearrangements during the aggregation process (Bayro et al. 2010). Despite all these detailed biophysical analyses on PI3-SH3, the NMR assignments of the ^{13}C nuclei, which provide exquisite structural information with regard to the protein secondary structure elements, have not been reported. Here we report the near complete NMR assignments of the 86-residue PI3-SH3 construct in its native state. These

Published online: 06 July 2013

NMR assignments are used to compare with the solid state NMR data of PI3-SH3 in its aggregated state. These data can also be used in the future to investigate conformational changes of PI3-SH3 under different conditions, such as the aggregation-prone, acid-denatured state.

Methods and experiments

Protein expression and purification

The expression and purification of the recombinant PI3-SH3 were carried out following the previously described procedures (Booker et al. 1993). Briefly, the recombinant PI3-SH3 was transformed into an *E. coli* expression strain and expressed as a glutathione S-transferase (GST) fusion protein with the tag fused at the N-terminus in minimum medium containing ^{15}N-labelled ammonium chloride (1 g/L) and ^{13}C-labelled D-glucose (3 g/L) as the sole nitrogen and carbon sources. The overexpressed recombinant protein was purified using a glutathione-Sepharose column followed by thrombin cleavage to separate the GST tag, a second glutathione-Sepharose column to remove the digested GST tag, and finally size-exclusion chromatography to purify the recombinant PI3-SH3 to homogeneity. Due to the design of the GST fusion construct, the N-terminus of the recombinant PI3-SH3 has an extension of a Gly-Ser dipeptide. The numbering of the NMR assignments in this study shall start with the two additional residues hereafter, i.e., the residue numbers of PI3-SH3 will plus two with respect to the original gene sequence. The recombinant protein was concentrated, flash-frozen by liquid nitrogen and stored at −20 °C until further use.

NMR spectroscopy

The NMR sample contains ca. 0.5 mM of U-[^{13}C,^{15}N] PI3-SH3 and buffered in 50 mM potassium phosphate (pH 6.0) with 10 % (v/v) D_2O for NMR lock signal. All NMR spectra of PI3-SH3 were acquired at 298 K on Bruker AVANCE spectrometers, which operate at a proton Larmor frequency of 500 MHz or 600 MHz, and are equipped with a cryogenic triple resonance probe. [^{15}N–^{1}H] HSQC, constant-time [^{13}C–^{1}H] HSQC and standard triple resonance experiments, including HNCO, HN(CA)CO, CBCA(CO)NH, HNCACB and HBHANH were recorded for backbone assignments including ^{13}Cα, ^{13}Cβ ^{1}HN, ^{13}C' and ^{15}N spin systems. For side-chain assignments, ^{15}N-edited NOESY-HSQC, ^{15}N-edited TOCSY-HSQC, aromatic [^{13}C–^{1}H] HSQC, (HB)CB(CECE)HE and (HE)CB(CGCDCE)HE, H(CCCO)NH, (H)C(CO)NH, H(C)CH-TOCSY and (H)CCH-TOCSY were recorded (Cavanagh et al. 2007; Sattler et al. 1999). Additionally, relaxation-optimised version of protonless CON, CACO and CBCACO spectra were

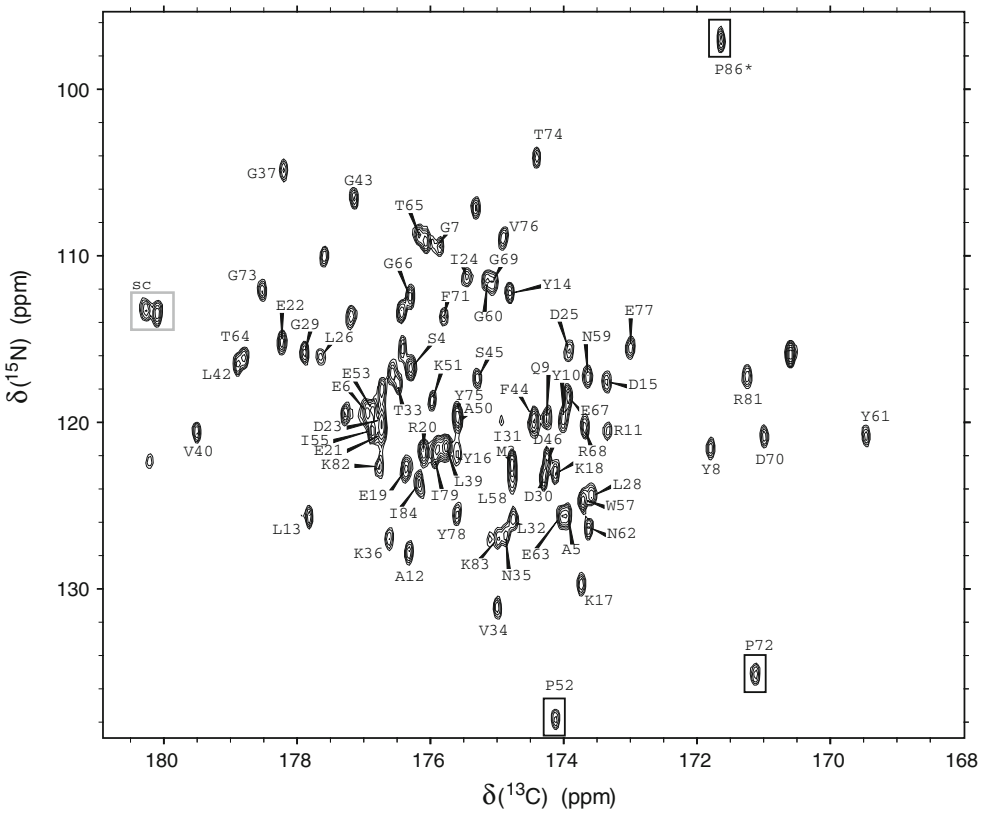

Fig. 1 Assigned protonless CON spectrum of PI3-SH3, recorded at 298 K, 14 Tesla. Each cross-peak in the CON spectrum correspond to the sequential connection of amide nitrogen of individual residues and the carbonyl carbon of the preceding residues (N_i–CO_{i-1}). For clarity, each cross-peak is labelled with the residue type and sequence of the amide nitrogen to which it corresponds. The three cross-peaks that correspond to P52, P72 and P86, which are not accessible to proton-based ^{15}N–^{1}H HSQC experiments are indicated in boxes. Note that the cross-peak of P86 is aliased along the nitrogen dimension. The amine nitrogen of P86 has a chemical shift value of 142.1 ppm

recorded (Bermel et al. 2009). All NMR data were processed and analysed by TopSpin (Bruker BioSpin), NMRPipe (Delaglio et al. 1995) and Sparky (Goddard and Kneller) software packages. The assignments procedure of the backbone resonances has been described previously (Hsu et al. 2009a, c).

Extent of assignments and data deposition

We have obtained complete backbone assignments (H^N, Hα, N, Cα, Cβ and C') of PI3-SH3 with the exception of the Gly residue at the N-terminus. The use of protonless NMR spectroscopy (Bermel et al. 2006a, b; Hsu et al. 2009b) was crucial in identifying of the amine nitrogen nuclei of proline residues that are otherwise inaccessible to conventional proton-based [^{15}N–^{1}H] HSQC spectroscopy. This also leads to the underrepresentation of the reported chemical shifts of the proline amine nitrogen nuclei. In the case of PI3-SH3, in particular, the C-terminus is a proline residue, which prohibits conventional sequential assignments. Using a combination of CON, CACO and CBCACO spectra, together with the prior knowledge that the chemical shifts of the C-terminal carbonyl carbons are generally much more down-field shifted, we managed to make a tentative assignment for the entire spin system of P86. Additionally the ^{15}N–^{1}H correlation corresponding to the second residue, Ser, at the N-terminus was missing in the [^{15}N–^{1}H] HSQC spectrum, most likely due to rapid solvent exchange. We therefore had to resort to the use of a combination of CON, CACO, CBCACO and [^{13}C–^{1}H] HSQC spectra to complete the assignment of the backbone assignments, expect the assignment for its H^N. Despite the lower sensitivity of the carbon-detection spectroscopy, the sensitivity of the commercial ^{13}C-optimised probe heads are sufficiently high to allow acquisition of high-quality 2D protonless spectra within a few hours which enable recovery of spectral information due to rapid solvent exchange (Hsu et al. 2009b) and the loss of sequential connectivities due to proline residues (Fig. 1). The PROSIAS webserver (http://www.nmr.chem.uu.nl/users/rob/prosias_setup_cgi.html), which uses protein sequence, backbone resonances, and the peaklists of [^{13}C–^{1}H] HSQC, H(CCCO)NH, (H)C(CO)NH, H(C)CH-TOCSY and (H)CCH-TOCSY, was used to aid the aliphatic side-chain assignments of PI3-SH3. For the assignments of the aromatic side-chains, the assignments were achieved manually using a combination of aromatic [^{13}C–^{1}H] HSQC, (HB)CB(CECE)HE and (HE)CB(CGCDCE)HE. The overall

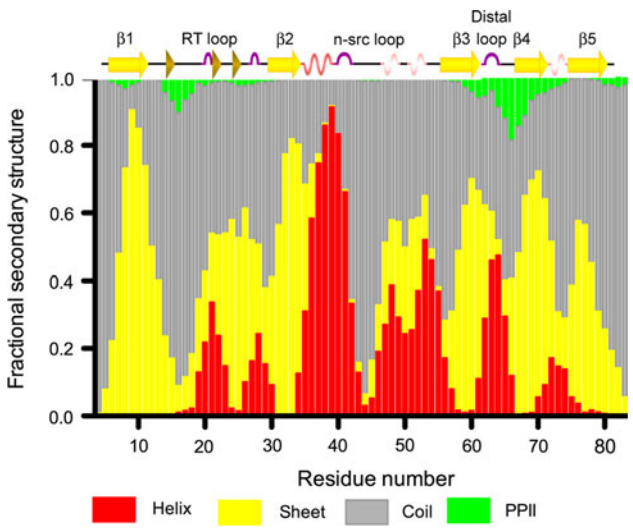

Fig. 2 Secondary structure population of PI3-SH3 calculated by its backbone chemical shifts. The fractional secondary structure populations of α-helix, β-sheet, random coil and polyproline II helix (PPII) are coloured *red*, *yellow*, *grey* and *green*, respectively, and the sum of these four equates to unity. For reference, the reported secondary structure elements, which have been determined by X-ray crystallography (PDB entry 1PHT) are shown on the *top*. The secondary structure populations are calculated by the δ2D webserver http://www-vendruscolo.ch.cam.ac.uk/d2D/ (Camilloni et al. 2012)

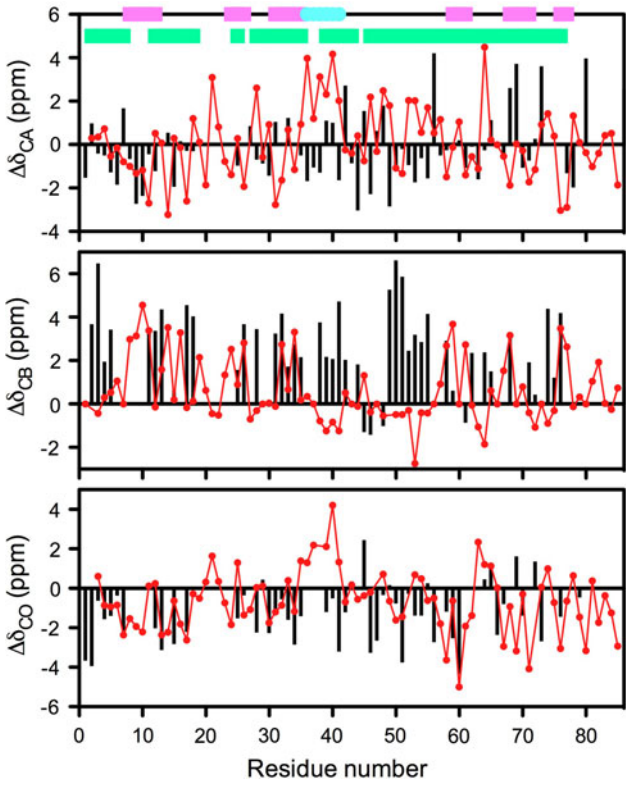

Fig. 3 Comparison of secondary chemical shifts of PI3-SH3 in its native (*red lines*) and fibrilar state (*black bars*). The top, middle and bottom panels show the secondary chemical shifts of CA, CB and CO, respectively. The random coil shifts are calculated using the CamCoil webserver http://www-vendruscolo.ch.cam.ac.uk/camcoil.php (De Simone et al. 2009). The residues that are β-stranded in the native and fibrilar states are indicated by *magenta* and *green bars*, respectively, on top of the panels. Additionally, the residues that are α-helical are indicated in a *cyan bar*. The secondary structure predictions are made by the δ2D webserver (Camilloni et al. 2012)

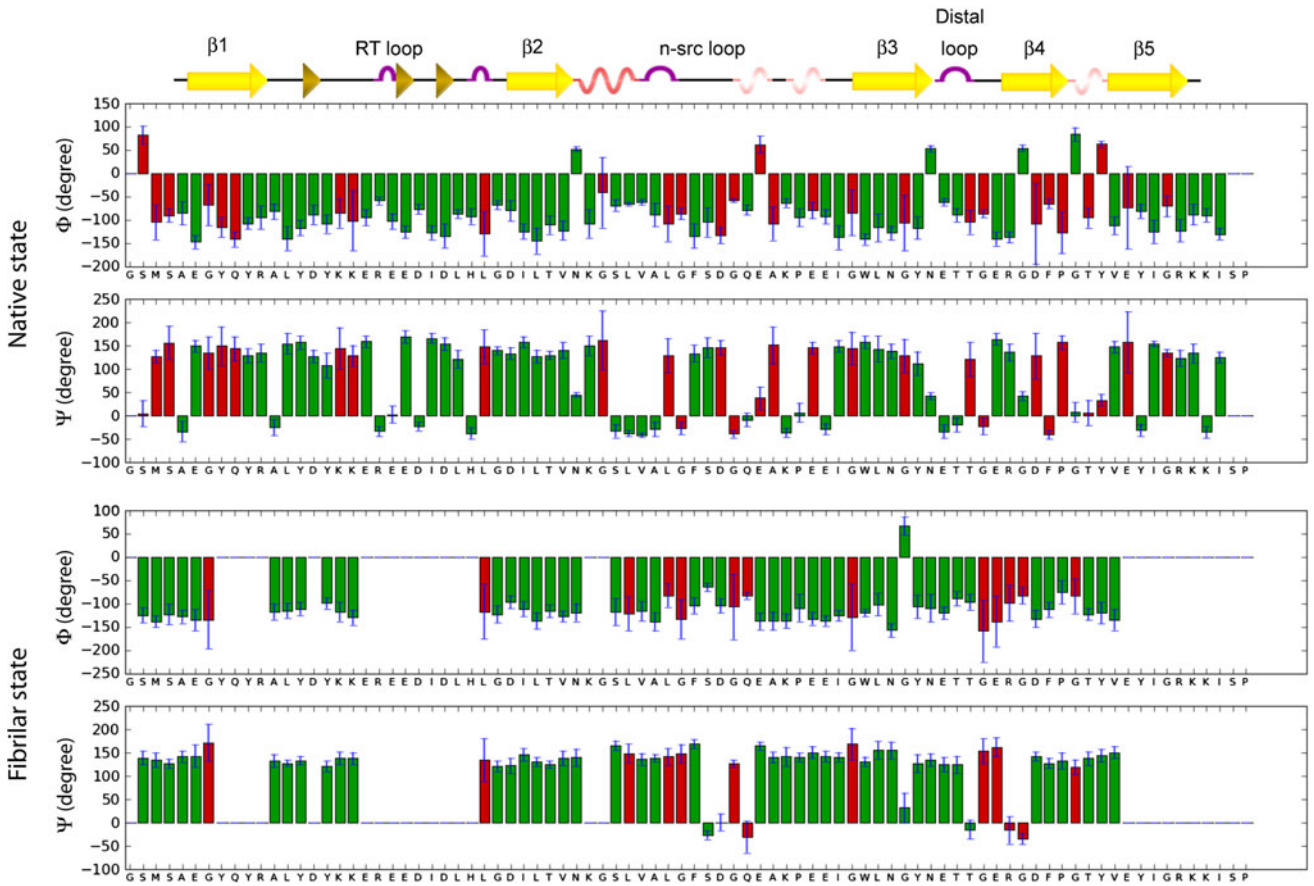

Fig. 4 Comparison of predicted backbone Φ/Ψ torsion angles of PI3-SH3 in its native (*upper panels*) and fibrilar state (*lower panels*). The predicted backbone Φ/Ψ torsion angles are calculated using the WeNMR TALOS + webserver (Shen et al. 2009; Wassenaar et al. 2012). *Green* and *red bars* indicate that the predictions are reliable and ambiguous, respectively

completeness of the side-chain resonances, excluding the labile groups, is more than 90 %. The NMR assignments are deposited to the BioMagResBank (http://www.bmrb.wise.edu/) under the accession code 19110.

Base on the assignment backbone resonances of PI3-SH3 under native condition, we calculated the secondary structure populations of individual amino acids as a function of protein sequence (Fig. 2). The exceptionally long n-src loop exhibits high helical content, which is consistent with earlier reports (Booker et al. 1993; Koyama et al. 1993a, b; Liang et al. 1996). We next compare our backbone ^{13}C chemical shifts of PI3-SH3 (Cα, Cβ and C′) in native state with those in amyloid state, which were assigned by the use of solid state NMR spectroscopy (Bayro et al. 2010). Except for residues 30–35 and 55–60, the backbone chemical shifts of native PI3-SH3 and its amyloid fibrilar counterpart are very different (Fig. 3), indicating that the amyloid formation is accompanied with significant conformational changes. Having said that, the predicted backbone torsion angles, Φ and Ψ (Shen et al. 2009), are rather similar, with the exception of those in the n-src and distal loops, which also adopt extended conformations in the amyloid fibrilar state (Fig. 4). Collectively, the results illustrate the importance of having the assignments of the backbone ^{13}C nuclei, which report not only the local secondary structures but tertiary structures thereby providing useful structural information for chemical shift-based structure calculations (Cavalli et al. 2007; Shen et al. 2008).

Acknowledgments We thank Dr Niel Birkett (University of Cambridge, UK) for the assistance in NMR sample preparation. The NMR spectra were obtained at the Biomolecular NMR facility, Department of Chemistry, University of Cambridge, UK and the Core Facility for Protein Structural Analysis supported by National Core Facility Program for Biotechnology, Taiwan. STDH is a recipient of the Career Development Award (CDA—00025/2010-C) from the International Human Frontier Science Program and is supported by funding from the National Science Council (100-2113-M-001-031-MY2 and 101-2627-M-001-004) and Academia Sinica, Taiwan.

References

Bayro MJ, Maly T, Birkett NR, MacPhee CE, Dobson CM, Griffin RG (2010) High-resolution MAS NMR analysis of PI3-SH3 Amyloid Fibrils: backbone conformation and implications for protofilament assembly and structure. Biochemistry 49:7474–7484

Bermel W, Bertini I, Felli IC, Lee YM, Luchinat C, Pierattelli R (2006a) Protonless NMR experiments for sequence-specific assignment of backbone nuclei in unfolded proteins. J Am Chem Soc 128:3918–3919

Bermel W, Bertini I, Felli IC, Piccioli M, Pierattelli R (2006b) ^{13}C-detected protonless NMR spectroscopy of proteins in solution. Prog NMR Spectrosc 48:24–45

Bermel W, Bertini I, Felli IC, Pierattelli R (2009) Speeding Up ^{13}C direct detection biomolecular NMR Spectroscopy. J Am Chem Soc 131:15339–15345

Booker GW, Gout I, Downing AK, Driscoll PC, Boyd J, Waterfield MD, Campbell ID (1993) Solution structure and ligand-binding site of the SH3 domain of the p85 alpha subunit of phosphatidylinositol 3-kinase. Cell 73:813–822

Camilloni C, De Simone A, Vranken WF, Vendruscolo M (2012) Determination of secondary structure populations in disordered states of proteins using nuclear magnetic resonance chemical shifts. Biochemistry 51:2224–2231

Cavalli A, Salvatella X, Dobson CM, Vendruscolo M (2007) Protein structure determination from NMR chemical shifts. Proc Natl Acad Sci USA 104:9615–9620

Cavanagh J, Fairbrother WJ, Palmer AG III, Rance M, Skelton NJ (2007) Protein NMR spectroscopy, 2nd edn. Academic Press, San Diego

De Simone A, Cavalli A, Hsu ST, Vranken W, Vendruscolo M (2009) Accurate random coil chemical shifts from an analysis of loop regions in native states of proteins. J Am Chem Soc 131: 16332–16333

Delaglio F, Grzesiek S, Vuister GW, Zhu G, Pfeifer J, Bax A (1995) NMRPipe: a multidimensional spectral processing system based on UNIX pipes. J Biomol NMR 6:277–293

Guijarro JI, Morton CJ, Plaxco KW, Campbell ID, Dobson CM (1998a) Folding kinetics of the SH3 domain of PI3 kinase by real-time NMR combined with optical spectroscopy. J Mol Biol 276:657–667

Guijarro JI, Sunde M, Jones JA, Campbell ID, Dobson CM (1998b) Amyloid fibril formation by an SH3 domain. Proc Natl Acad Sci USA 95:4224–4228

Hsu ST, Behrens C, Cabrita LD, Dobson CM (2009a) 1H, 15 N and ^{13}C assignments of yellow fluorescent protein (YFP) Venus. Biomol NMR Assign 3:67–72

Hsu ST, Bertoncini CW, Dobson CM (2009b) Use of protonless NMR spectroscopy to alleviate the loss of information resulting from exchange-broadening. J Am Chem Soc 131:7222–7223

Hsu ST, Cabrita LD, Christodoulou J, Dobson CM (2009c) 1H, 15 N and ^{13}C assignments of domain 5 of Dictyostelium discoideum gelation factor (ABP-120) in its native and 8 M urea-denatured states. Biomol NMR Assign 3:29–31

Jimenez JL, Guijarro JI, Orlova E, Zurdo J, Dobson CM, Sunde M, Saibil HR (1999) Cryo-electron microscopy structure of an SH3 amyloid fibril and model of the molecular packing. EMBO J 18:815–821

Koyama S, Yu H, Dalgarno DC, Shin TB, Zydowsky LD, Schreiber SL (1993a) 1H and 15 N assignments and secondary structure of the PI3 K SH3 domain. FEBS Lett 324:93–98

Koyama S, Yu H, Dalgarno DC, Shin TB, Zydowsky LD, Schreiber SL (1993b) Structure of the Pl3 K SH3 domain and analysis of the SH3 family. Cell 72:945–952

Liang J, Chen JK, Schreiber SL, Clardy J (1996) Crystal structure of P13 K SH3 domain at 2.0 $\sqrt{}$Ö resolution. J Mol Biol 257: 632–643

Orte A, Birkett NR, Clarke RW, Devlin GL, Dobson CM, Klenerman D (2008) Direct characterization of amyloidogenic oligomers by single-molecule fluorescence. Proc Natl Acad Sci USA 105: 14424–14429

Sattler M, Schleucher J, Griesinger C (1999) Heteronuclear multidimensional NMR experiments for the structure determination of proteins in solution employing pulsed field gradients. Prog Nucl Magn Reson Spectrosc 34:93–158

Shen Y, Lange O, Delaglio F, Rossi P, Aramini JM, Liu G, Eletsky A, Wu Y, Singarapu KK, Lemak A et al (2008) Consistent blind protein structure generation from NMR chemical shift data. Proc Natl Acad Sci USA 105:4685–4690

Shen Y, Delaglio F, Cornilescu G, Bax A (2009) TALOS+: a hybrid method for predicting protein backbone torsion angles from NMR chemical shifts. J Biomol NMR 44:213–223

Ventura S, Lacroix E, Serrano L (2002) Insights into the origin of the tendency of the PI3-SH3 domain to form Amyloid Fibrils. J Mol Biol 322:1147–1158

Wassenaar T, Dijk M, Loureiro-Ferreira N, Schot G, Vries S, Schmitz C, Zwan J, Boelens R, Giachetti A, Ferella L et al (2012) WeNMR: structural biology on the grid. J Grid Comput 10: 743–767

Zurdo J, Guijarro JI, Jiménez JL, Saibil HR, Dobson CM (2001) Dependence on solution conditions of aggregation and amyloid formation by an SH3 domain. J Mol Biol 311:325–340